Diffusivity and Conductivity of a Solvent Primitive Model Electrolyte in a Nanopore by Equilibrium and Nonequilibrium Molecular Dynamics Simulations

Yuk Wai Tang,[†] István Szalai,[‡] and Kwong-Yu Chan*[,†]

Department of Chemistry, The University of Hong Kong, Pokfulam Road, Hong Kong SAR, China, and Department of Physics, University of Veszprém, P.O. Box 158, H-8201 Veszprém, Hungary

Received: January 31, 2001; In Final Form: June 1, 2001

Equilibrium and nonequilibrium molecular dynamics simulations are performed to calculate the diffusion coefficient and electric conductivity of ions in a 0.1 M concentration solution confined in neutral cylindrical pores. The applied model is a solvent primitive model (SPM) in which both ions and solvent molecules are soft core spheres and the polar nature of the solvent is represented implicitly as a background with a given dielectric constant. The simulations are carried out in an isokinetic ensemble, and the system, responsing to an applied electric field, is maintained at constant temperature by a Gaussian thermostat. From equilibrium molecular dynamics, diffusion coefficients of ions and solvent decrease with decreasing pore radius or increasing packing fraction of solvent particles. The conductivity determined by nonequilibrium molecular dynamics shows a similar trend, but the pore-size dependence of conductivity does not have a local maximum as was found in the restricted primitive model in which solvent spheres are absent. Using the Nernst−Einstein relation, the ionic conductivity is also calculated from the equilibrium diffusion coefficient and compared with the conductivity obtained from nonequilibrium simulations. The comparison shows that the Nernst−Einsten relation is not valid only at low solvent packing and in very small pores.

Introduction

The physical properties of electrolytes confined in nanostructures are expected to be significantly different from those in the bulk state. The prediction and determination of confined electrolytes properties are important in biology, materials science, and electrochemistry. Two typical examples are to understand the biological processes controlled by channels in membranes and to optimize performance of fuel cells which are dependent on Nafion membranes and porous electrodes. Limited experimental data have been reported for fluids confined in nanopores,[1] and the properties of confined fluids have been mainly studied using integral equation theories and computer simulations.[2] Anomalies for simple fluids are found in compression of the phase envelopes[3] and decrease in transport properties.[4] Studies of the equilibrium properties of electrolytes confined in nanopores have been reported recently. Most of the theoretical and simulation studies of electrolytes adsorption were based on the primitive model (PM) using a continuum dielectric background to represent the solvent.[5−13] The focus has been on the amount of counterions and co-ions adsorbed or how much salt in excluded. The ion selectivity in a biological ion channel has been demonstrated with the primitive model.[13] Simulation of a more realistic molecular solvent model, the solvent primitive model (SPM) confined in a nanopore, has recently been reported.[14]

Transport properties of confined electrolytes are of greater technological importance. Conductivity in perfluorosulfonic acid membranes has been measured by ac impedance methods.[15,16] The interpretation of results has been hampered by the poor characterization of the membrane structure, and definitive measures of membrane pore sizes are lacking. Westerman-Clark and Anderson[17] measured conductivity of various electrolytes in track-etched mica membranes. Hansma et al.[18] reported conductance through a single submicrometer diameter pore using a scanning ion-conductance microscope. These techniques, however, are difficult for pores a few nanometers in diameters. In biophysics, the patch-clamp technique of Sackmann and Neher[19] is widely used to determine the current−voltage characteristics of various ion channels in different electrolytes. Molecular dynamics (MD) simulations are valuable for the interpretation of these experimental data and to explore situations not accessible by experiments. Some limited equilibrium molecular simulation (EMD) data in the restricted primitive model (RPM) were reported by Lo et al.[12] for charged nanopores. The restricted primitive model means the ions are of the same size in the primitive model. Lynden-Bell and Rasaiah reported EMD simulation of sodium ions and simple point charge (SPC) solvent in neutral nanopores of various sizes.[20] Various EMD simulations for realistic biological ion channels have also been reported.[21,22] While it is difficult to simulate realistic atomistic channels for long times to compare with patch-clamp experiments, the strategy has been to obtain short time diffusion coefficients using EMD and applied this to predict current in a nonequilibrium situation. This is in accordance of the Nernst−Plank theory of ionic flux and the Nernst−Einstein theory of ionic conductivity. The validity of this approach has to be tested by comparing EMD and nonequilibrium molecular dynamics simulations (NEMD). Applications of NEMD in the restricted primitive model have been reported for the bulk phase[23,24] and recently in nanopores.[25] Tang et al.[25] found the anomaly of higher conductivity in a nanopore for a RPM electrolyte. They also found a discrepancy between EMD-projected conductivity based on Nernst−Einstein theory and the conductivity obtained

* Corresponding author. E-mail: hrsccky@hku.hk. Fax: (852) 2857-1586.
[†] The University of Hong Kong.
[‡] University of Veszprém. E-mail: szalai@almos.vein.hu.

10.1021/jp010414u CCC: $20.00
Published on Web 09/26/2001

in NEMD simulations. In this paper, EMD and NEMD simulations for a more realistic solvent primitive model (SPM) electrolyte in an infinitely long neutral nanopore are reported. Comparison between the EMD and NEMD results will be discussed in the light of Nernst−Einstein and Nernst−Planck theories. Comparison with the results of RPM model[25] will also be made. While several earlier studies[8−12,14] have focused on charged pores and electroneutrality, this paper will only report studies of uncharged nanopores.

Model and Simulation Method

In the SPM, the ions are modeled by charged hard spheres while the solvent molecules are neutral hard spheres. The polar nature of the solvent is represented implicitly by a continuum background with a dielectric constant ϵ_r. To avoid the technical inconvenience caused by a noncontinuous interaction potential in the molecular dynamics simulation, a soft sphere potential is used to describe the core of ions and solvent molecules. The soft sphere pair potential here is a Weeks−Chandler−Anderson-type shifted Lennard-Jones (LJ) potential given as

$$u_{\alpha\beta}^{ss}(r_{ij}) = \begin{cases} 4\epsilon_{\alpha\beta}\left[\left(\frac{d_{\alpha\beta}}{r_{ij}}\right)^{12} - \left(\frac{d_{\alpha\beta}}{r_{ij}}\right)^{6}\right] + \epsilon_{\alpha\beta} & r_{ij} \le r_{min}(\alpha,\beta) \\ 0 & r_{ij} > r_{min}(\alpha,\beta) \end{cases} \quad (1)$$

where r_{ij} is the distance between two species i and j and $\epsilon_{\alpha\beta}$ and $d_{\alpha\beta}$ are the energy and distance parameters of the potential, which can be defined by the corresponding single particle parameters using the Lorentz−Berthelot combining rules. These α and β subscripts can be +, −, or s, representing either the cation, anion, or the solvent, respectively. The distance $r_{min}(\alpha,\beta) = 2^{1/6}(d_{\alpha\alpha} + d_{\beta\beta})/2$ is the location of minimum of the untruncated LJ potential prior to the shifting and depends on the sizes of interacting particles. The electrostatic interaction between an ion pair in a continuum solvent of dielelectric constant ϵ_r is given by the Coulomb pair potential

$$u_{\alpha\beta}^{C}(r_{ij}) = \frac{q_i q_j}{4\pi\epsilon_0\epsilon_r r_{ij}} \quad (2)$$

where q_i and q_j are the electrostatic charges of ions and ϵ_0 is the dielectric permittivity of vacuum. Using eqs 1 and 2, the total interaction potential in the framework of SPM can be given by two equations, first for the ion−ion interaction as

$$u_{\alpha\beta}^{SPM}(r_{ij}) = u_{\alpha\beta}^{ss}(r_{ij}) + u_{\alpha\beta}^{C}(r_{ij}) \quad (3)$$

and second for the ion−solvent and solvent−solvent interaction

$$u_{\alpha\beta}^{SPM}(r_{ij}) = u_{\alpha\beta}^{ss}(r_{ij}) \quad (4)$$

Particles are confined in a cylindrical cell of radius R and length H. The ion−wall and solvent−wall interactions are described by a soft particle−soft wall interaction potential. No Coulomb interaction is present between the ions and the wall since the wall is uncharged. The dielectric constant of the wall and the outside region is assumed to be the same as water. This simplification will avoid the need of solving the electrostatic boundary conditions of regions of different dielectric constants. The shifted LJ type wall potential proposed by Tjatjopoulos et al.[26] was adopted and given as

$$u_{w\alpha}(r_i) = \begin{cases} u_{w\alpha}^{LJ}(r_i) + u_{w\alpha}^{LJ}(r_{wmin}) & r_i \ge r_{wmin}(w,\alpha) \\ 0 & r_i < r_{wmin}(w,\alpha) \end{cases} \quad (5)$$

where

$$u_{w\alpha}^{LJ}(r_i) = n_w\epsilon_{w\alpha}\pi^2\left\{\frac{63}{32}\frac{1}{(R/d_{w\alpha} - r_i/d_{w\alpha})^{10}((R + r_i)/R)^{10}}F\left[-\frac{9}{2}, -\frac{9}{2}, 1, (r_i/R)^2\right] - 3\frac{3}{(R/d_{w\alpha} - r_i/d_{w\alpha})^{4}((R + r_i)/R)^{4}}F\left[-\frac{3}{2}, -\frac{3}{2}, 1, (r_i/R)^2\right]\right\} \quad (6)$$

Here n_w is the reduced surface number density of the wall, $d_{w\alpha}$ and $\epsilon_{w\alpha}$ are the distance and energy parameters of the wall particle interaction, r_i is the radial distance of ith particle from the center of the cylinder, $r_{w\ min}(w,\alpha)$ is the location of the minimum of the LJ wall potential, and $F[\alpha, \beta, \gamma, x]$ denotes the corresponding hypergeometrical function. The Lorentz−Berthelot combining rules are also used to determine the wall−particle interaction parameters. The corresponding wall forces can be derived analytically using the differentiation rules of hypergeometrical functions.[27]

Equilibrium Molecular Dynamics Simulation. NVT ensemble (isokinetic) equilibrium molecular dynamics simulations were performed, in which the temperature of the system is kept at a fixed value by a Gaussian thermostat. The equations of motion were integrated using a modified Verlet algorithm.[28] Periodic boundary conditions are applied only in the axial direction, designated as the z direction. The axial diffusion coefficient of different species (D_α) was calculated on the basis of the Einstein relation

$$D_\alpha = \frac{1}{2}\lim_{t\to\infty}\frac{\langle|z_{\alpha i}(t) - z_{\alpha i}(0)|^2\rangle}{t} \quad (7)$$

where the brackets $\langle ... \rangle$ denote the ensemble average of the mean axial displacement of α type species. Strictly speaking, mutual diffusion coefficients should be considered in the SPM model, which is of a mixture of three species. The analyses of MacElroy and Suh[29] can be adapted to compute the diffusion coefficients in a mixture and relate them to individual fluxes. Simplifications can be made, however, when a species is at infinite dilution and only self-diffusion coefficients are required to compute the fluxes. At the 0.1 M concentration, the ion species is dilute compared to the solvent and we assume that only the self-diffusion coefficient of (7) is needed to compute the diffusion of ions. To calculate the diffusion coefficients according to eq 7, the knowledge of the real position of particles is necessary. To eliminate the effect of the periodic boundary condition from the z displacement, the method given by Rapaport[28] is used. Because in this work we studied the SPM at low ion concentration, we did not use any long-range correction to the electrostatic forces, as discussed previously.[25]

Nonequilibrium Molecular Dynamics Simulation. To study the electric migration of ions in the framework of SPM, nonequilibrium molecular dynamics simulations are performed with a technique described previously.[25] A constant uniform electric field, E_z, is applied in the axial direction of the cylindrical pore. Under the field, the charged particles move and generate an average current after some simulation steps. The ionic concentration of the simulation cell is maintained constant by the axial periodic boundary condition. This method has the advantage of generating a constant flux of ions without

TABLE 1: Parameters in the SPM Model

species	symbol	q/e	(ϵ/k)/K	d/Å	m/au
cation	+	+1	316.35	3.0	23
anion	−	−1	316.35	3.0	23
solvent	s	0	78.20	3.0	18
wall	w	0	316.35	3.0	•

the need of a dual control volume grand canonical molecular dynamics (DCVGCMD) simulation.[30] In addition the correction of interdependent diffusion by the darken factor and consideration of osmotic effects will not be required. This simple technique, however, only studies electric migration of ions. The DCVGCMD or other similar methods will still be required to study transport of ions under a concentration gradient with or without an electric potential gradient. Although the absolute value of electric potential changes in the image cells, this has no effect in the molecular dynamics simulation as long as the field is uniform along the infinitely long pore. Since the external electric field does ohmic work on the system, the generated heat has to be removed to maintain a constant temperature. To solve this problem, we used NEMD method first proposed by Evans and Morris[31,32] and later applied to bulk[23,24] and confined electrolytes.[25] Here, the solution of the non-Newtonian equations of motion is not detailed and can be found in our previous publication.[25] A similar NEMD technique to calculate the direct current through an ion channel in a biological membrane has also been reported recently.[33]

The numerical integration of equations of motion is carried out by a modified Verlet algorithm, which was suggested by Heyes.[34,35] The definition of the electric current density in the axial direction (J_z), induced in response to the electric field E_z, is

$$J_z = \frac{1}{V}\sum_{j=1}^{N_i} q_j v_{j,z} \tag{8}$$

where $v_{j,z}$ is the axial component of the velocity of jth ion, V is the volume of the pore, and N_i is the total number of ions. In the linear response range, the electric conductivity (σ) can be defined by a simple limit as

$$\sigma = \lim_{E_z \to 0} \frac{J_z}{E_z} \tag{9}$$

To calculate the electric conductivity, a linear extrapolation based on the above equation is used.

Parameters of the Model and the Simulations. We studied a symmetric, univalent 1:1 electrolyte whose concentration was $c \cong 0.1$ mol/dm^3. All simulations reported here were carried out at $T = 298.15$ K. For the dielectric constant of the solvent $\epsilon_r = 78.3$ was used, which is the relative permittivity of water at the given temperature. Without loss of generality, the cations, anions, and solvent particles are all given the same size. The applied potential parameters are summarized in Table 1. The mass and energy parameters of ions are chosen to resemble sodium ion whereas those of the solvent resemble water. The anion symmetrical to the cation does not resemble any realistic ion. The reduced surface number density of the wall potential was chosen to be $n = 1$. At the integration of equations of motion for the size of the reduced time step $\Delta t/\tau = 0.001$ was used with $\tau = d_+\sqrt{m_+/\epsilon_+}$, where the sign + refers to the parameters of the positive ion. Both EMD and NEMD simulations were carried out at two different solvent packing fractions: at $\eta_s = 0.2$ and $\eta_s = 0.3$, where $\eta_s = (\pi N_s d_s^3)/6V$. The pore-size dependence of simulation results were also investigated. The simulation parameters, including the particle numbers, are summarized in Table 2

TABLE 2: Parameters of EMD and NEMD Simulation Runs[a]

pore size $(R/d)\times(H/d)$	η_s	no. of particles (N_s, N_+, N_-)	no. of time steps after equilib	no. of time steps for NEMD
3 × 322	0.2	2817, 12, 12	10 000 000	10 000 000
3 × 322	0.3	4225, 12, 12	10 000 000	10 000 000
4 × 172	0.2	2826, 12, 12	10 000 000	10 000 000
5 × 106	0.2	2810, 12, 12	10 000 000	10 000 000
5 × 106	0.3	4213, 12, 12	10 000 000	10 000 000
7.5 × 91	0.2	5661, 24, 24	10 000 000	10 000 000
7.5 × 91	0.3	8491, 24, 24	10 000 000	10 000 000
10 × 79	0.2	8920, 38, 38	10 000 000	10 000 000
10 × 79	0.3	13 380, 38, 38	10 000 000	10 000 000
15 × 102	0.2	26 810, 114, 114	5 000 000	2 000 000
15 × 102	0.3	40 216, 114, 114	5 000 000	2 000 000

[a] $\eta_s = (\pi/6)N_s d_s^3/V$ is the packing fraction of solvent particles.

Nernst−Planck and Nernst−Einstein Equations

Most of the reported molecular dynamics simulations of ion transport in channels[20−22] are based on equilibrium simulations. To predict the current through the ion channel or a membrane, the phenomenological Nernst−Planck equation[36,37] is applied to calculate the flux of each ion. The Nernst−Planck equation can be expressed in one dimension as

$$N_\alpha = -D_\alpha \frac{dc_\alpha}{dz} - \frac{z_\alpha e D_\alpha c_\alpha}{kT}\frac{d\phi}{dz} + c_\alpha v_z \tag{10}$$

where N_α is the flux of ion species α in the z direction, z_α is its charge valance, c_α is the ion concentration of α, e is the elementary charge, v_z is the velocity in the z direction due to convection, ϕ is the electric potential, and k is the Boltzmann constant. A more general equation should use chemical potential gradients and include mutual diffusion terms in a mixture. Equation 10 has neglected the flux caused by the concentration gradients of other components in the solution. As discussed earlier in the context of eq 7, the density of a dilute ionic solution is dominated by the solvent and mutual diffusion is negligible. Furthermore, our discussion will focus on migration of ions in the absence of macroscopic concentration or chemical potential gradients and cross diffusion can be ignored. The current density is expressed by a sum of the fluxes of charges as

$$J_z = \sum_\alpha e z_\alpha N_A N_\alpha \tag{11}$$

where N_A is the Avogadro number. Equation 10 is based on a macroscopic linear gradient theory and required the input of the diffusion coefficient for the migration term. The practically achievable time and length scales of molecular simulation still fall short of experimentally measurable magnitudes by orders of magnitude. The strategy of a predictive approach has been to calculate the diffusion coefficient using short time or short length scale EMD simulations and apply a macroscopic theory like the Nernst−Planck eq 10 to compute fluxes in a nonequilibrium situation. This approach has also been extended to treat the space charges of protein by combining the use of Poisson's equation, referred to as the Poisson−Nernst−Planck equations.[22] The validity of this approach is expressed more concisely by the Nernst−Einstein relation,[38]

$$\sigma = \frac{e^2 N_A}{kT} \sum_\alpha z_\alpha{}^2 c_\alpha D_\alpha \tag{12}$$

In other words, the electrical conductivity calculated from the current response to an electric field can be related to equilibrium diffusion coefficient. It is well-known that the Nernst−Einstein equation is correct in dilute solutions. At higher electrolyte concentration, discrepancy to eq 12 arises due to association or other ion−ion interaction and ion fluxes are not independent of each other. The effect of confinement in nanostructures on the validity of the Nernst−Einstein and Nernst−Planck or Poisson−Nernst−Planck framework, however, has not been investigated.

One of the tasks of our work is to study the validity of the Nernst−Einstein relation in electrolytes confined in a cylindrical pore. In parallel to the EMD simulations, NEMD simulations are performed to calculate current densities and conductivities of the SPM electrolyte. For a symmetric, univalent 1:1 electrolyte, eq 12 in reduced units can be simplified to

$$\sigma^* = \frac{D_+{}^* \rho_I{}^*}{T^*} = \frac{D_-{}^* \rho_I{}^*}{T^*} \tag{13}$$

where $\sigma^* = \sigma d_+{}^2 \sqrt{m_+ \epsilon_+}/e^2$ is the reduced electric conductivity, $D_\alpha{}^* = D_\alpha / d_+{}^2 \epsilon_+ / m_+$ is the reduced diffusion coefficient of cations and anions, $\rho_I{}^* = (N_+ + N_-) d^3/V$ is the reduced density of all ions, and $T^* = (kT)/\epsilon_+$ is the reduced temperature. Because the potential parameters of the cation and anion are the same (except the sign of the charge; see Table 1), therefore the diffusion coefficients of these species must be equal in the framework of SPM and as well as RPM.

Results and Discussion

Cross-Sectional Area of the Nanopore. As mentioned in our previous publication,[25] the definition of the cross section of a simulation cell bounded by a soft wall is not trivial and requires some careful analysis. The issue is important because the volume of the pore is needed to calculate the concentration of ions, density of particles, and current density. In the EMD simulation of a pore with $R = 10d$ and $H = 77d$ using $N_s = 13311$, $N_+ = 38$, and $N_- = 38$ particles, the radial density distribution shows that the centers of particles are distributed in a cylinder of radius $R - 0.8d$, and outside this cylinder, practically no particles are found. The physical radius of the pore should therefore be $R_p = R - 0.3d$. The physical volume of our simulation cell is $V = (R - 0.3d)^2 \pi H$. For other pore sizes, we obtained similar results. Figure 1 shows the pore radius dependence of the density distribution at $\eta_s = 0.3$ solvent packing fraction in EMD simulations. It can be seen that there are very sharp peaks at half ionic diameter away from the above-defined physical pore radius. The heights of contact peak increases with decreasing pore radius, which is in agreement with the theoretical findings.[4,38,39] The correct definition of the physical pore limits is therefore important, particularly for very small pores.

Diffusion Coefficients from EMD. Diffusion coefficients for ions and solvent molecules are calculated in the EMD simulations according to eq 7 for different pore sizes and are summarized in Table 3 in reduced units. In several selected runs, separate calculations of diffusion coefficients from velocity autocorrelation functions give the same results. The pore-size dependence of diffusion coefficients is displayed in Figure 2. In all cases, the reduced density of all ions is $\rho_I{}^* \cong 0.00325$,

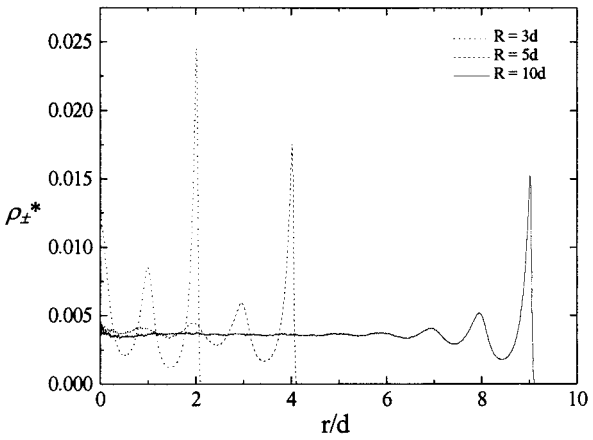

Figure 1. Equilibrium distributions of ions inside cylindrical pores at $\eta_s = 0.3$ solvent packing fraction.

corresponding to a symmetric electrolyte concentration of $c \cong 0.1$ M. Since the ions are modeled to have identical molecular parameters except the sign of their charges, their diffusion coefficient values should be the same in the overall neutral environment. In the EMD, we calculate separately the diffusion coefficients of positive and negative particles. The difference in their diffusion coefficients is only due to statistical uncertainties. In Figure 2, the average between the cation and anion diffusion coefficients is shown. The relative statistical uncertainty of reduced diffusion coefficient of ions is 3−8% depending on the pore size. The higher uncertainty for a smaller pore is due to the smaller number of charged particles (see Table 2). In the case of solvent molecules, the statistical uncertainty of diffusion coefficient is less then 1%. Figure 2 shows that the reduced diffusion coefficient of solvent particles is in general higher than that of ions, mainly because the mass of solvent particles is chosen to be lighter than that of the ions. Results of the RPM at the same electrolyte concentration are also included for comparison with the SPM results. As expected, the diffusion coefficient decreases with increasing packing fraction. The diffusion coefficients of ions modeled by the SPM at $\eta_s = 0.3$ are lower than those of the RPM by 2 orders of magnitude and are closer to experimental values. The SPM results at $\eta_s = 0.3$, however, are still 1 order of magnitude higher than the corresponding experimental values for simple aqueous electrolytes which have packing fractions higher than 0.4. The pore-size dependence of diffusion coefficients can be explained by the inhomogeneous concentration distribution in the pores (Figure 1). Theoretical results[4,38,39] explain that higher local concentration results in a lower local diffusion coefficient, which gives lower pore-averaged diffusion coefficients. As shown Figure 1 for the density profile of SPM at $\eta_s = 0.3$, the inhomogeneity increases with a smaller pore and the corresponding EMD diffusion coefficient obtained is smaller. The decrease of equilibrium diffusion coefficient of solvent with pore size is in qualitative agreement with previous results of Lynden-Bell infinite dilution using the simple point charge model (SPC/E) solvent.[20]

Conductivity of Ions from NEMD. The NEMD results are tabulated in Table 3 against the EMD results with the same pore and electrolyte parameters. The RPM results of $\eta_s = 0$ are from earlier reported.[25] For each value of conductivity, separate simulations at three different field strengths are used with reduced values of $E_z{}^* = 0.1$, 0.15, and 0.2 where $E_z{}^* = (ed_+/\epsilon_+)E_z$. The electric conductivity was calculated from the steady-state total current density response. From the field dependence of the electric conductivity, the equilibrium value (zero-field

TABLE 3: Transport Properties of 0.1 M 1:1 RPM/SPM Electrolyte from EMD and NEMD Simulations[a]

		EMD				NEMD		
η_s	R/d	D_+*	D_-*	D_s*	$D^*\rho^*/T^*$	U_c*	I_z* at $E^* = 0.2$	σ^*
0.0	1.5						5.68×10^{-4} ($E^* = 0.02$)	77.4×10^{-4}
0.0	2						0.0113 ($E^* = 0.02$)	767.3×10^{-4}
0.0	3	13.48	12.31		444.9×10^{-4}	−0.243	0.0293 ($E^* = 0.02$)	825.5×10^{-4}
0.0	5	15.57	15.86		542.1×10^{-4}	−0.261	0.0836 ($E^* = 0.02$)	599.0×10^{-4}
0.0	10	18.47	18.76		642.1×10^{-4}	−0.280	0.329 ($E^* = 0.02$)	537.3×10^{-4}
0.0	15	18.52	19.27		659.7×10^{-4}	−0.279	0.753 ($E^* = 0.02$)	550.0×10^{-4}
0.20	3	0.216	0.208	0.250	7.47×10^{-4}		1.67×10^{-3}	4.73×10^{-4}
0.20	4	0.268	0.264	0.300	9.26×10^{-4}	−0.224	6.66×10^{-3}	7.86×10^{-4}
0.20	5	0.285	0.289	0.328	10.1×10^{-4}	−0.261	0.0125	8.29×10^{-4}
0.20	7.5	0.309	0.322	0.361	10.9×10^{-4}	−0.274	0.0323	9.62×10^{-4}
0.20	10	0.308	0.328	0.375	11.0×10^{-4}	−0.282	0.0612	9.16×10^{-4}
0.20	15	0.344	0.332	0.375	11.9×10^{-4}	−0.284	0.142	10.00×10^{-4}
0.30	3	0.0921	0.0916	0.106	3.22×10^{-4}	−0.110	1.35×10^{-3}	2.28×10^{-4}
0.30	5	0.131	0.135	0.154	4.64×10^{-4}	−0.263	5.78×10^{-3}	4.32×10^{-4}
0.30	7.5	0.150	0.141	0.178	5.01×10^{-4}	−0.284	0.0160	4.54×10^{-4}
0.30	10	0.161	0.160	0.187	5.55×10^{-4}	−0.281	0.0308	4.32×10^{-4}
0.30	15	0.169	0.167	0.188	5.87×10^{-4}	−0.305	0.0704	4.57×10^{-4}

[a] $D_+^* = D_+(d^2\epsilon/m)^{-1/2}$, and D_-* and D_s* are similarly defined. $\rho_I^* = \rho_+^* + \rho_-^*$ is the total ions reduced density. $U_c^* = U_c/(N\epsilon)$ is the Coulomb energy per particle reduced to the Lennard-Jones energy parameter. $I_z^* = J_z^*\pi(R - 0.3d)^2/d^2$ is reduced current measured at a reduced electric field $E_z^* = E_z de/\epsilon$. $\sigma^* = \sigma d^2(me)^{1/2}/e^2$ is reduced conductivity.

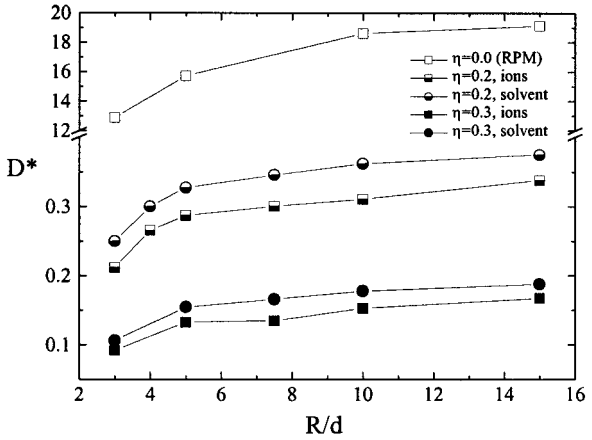

Figure 2. Reduced diffusion coefficients as a function of pore size of SPM particles at different solvent packing fractions corresponding to 0.1 M electrolyte concentration obtained by EMD simulations.

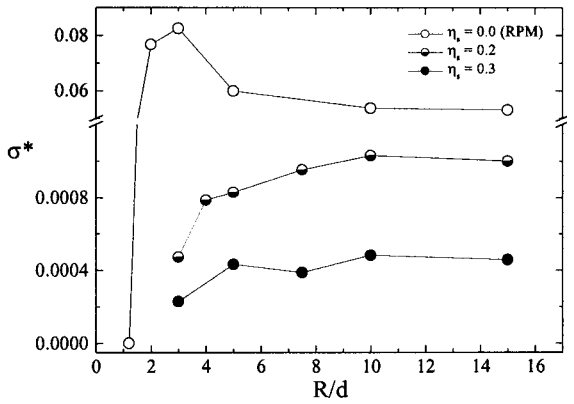

Figure 3. Reduced electric conductivity of SPM as a function of pore size in comparison with the corresponding RPM results at different solvent packing fractions obtained by NEMD simulations. (The data point of $R = 1.5d$ in Table 3 is not shown due to the break of the axis.)

value) was estimated by a linear extrapolation.[25] Because of the possible ambiguity of the cross-sectional area and volume of the nanopore, the reduced current I_z* is also tabulated in Table 3. The reduced electric conductivity in pores of different radii is displayed in Figure 3for the 0.1 M electrolyte at three different solvent packing fractions. The relative statistical error of electric conductivity is 5−15% and is larger for a smaller pore size. As in the case of EMD diffusion coefficients, the values of conductivity in the SPM are lower by approximately 2 orders of magnitude than the corresponding RPM values. It is evident that the drop in the conductivity is caused by the collision of the conducting ions with the nonconducting solvent molecules. Figure 3 shows that the electric conductivity of the SPM electrolyte decreases with decreasing pore radius, while that of RPM increases first before decreasing rapidly at very narrow pore size. Apparently, the electric conductivity of RPM electrolyte exhibits a local maximum. The increase of conductivity of the RPM electrolyte was explained by the weakening of the Coulomb interaction of the ions with decreasing pore size.[25] The average Coulombic energies of the ions are tabulated in Table 3 and are less negative for smaller pores due to the decrease of linear density of ions in the axial direction. The average Coulombic energy in Table 3 is reduced to the Lennard-Jones energy parameter and defined as $U_c^* = U_c/(N_i\epsilon_+)$. For pores with a radius less than 1.5d, oppositely charged ions, moving in opposite directions, are not able to get around each other. Therefore, the conductivity decreases rapidly with pore sizes less than 1.5d, even though the Coulombic interaction is weak. In the case the SPM electrolyte, the Columbic interaction energy becomes less negative with smaller pore size in a similar fashion, as shown in Table 3, and conductivity does not increase with decreasing pore size. It is obvious that collisions and inhomogeneity effects dominate over the Columbic interaction at the high packing fractions of the SPM electrolyte. As expected, the dc (direct current) conductivity of SPM will tend to zero with further decrease in the pore size because in a narrow pore the positive and negative ions are not able to get around each other. In the NEMD simulation of SPM, the external field applied was 10 times larger than in RPM to get reasonable currents. The modeled systems are packed with particles, and therefore, the movement of ions is in large extent hindered by the solvent particles. Small field strength results in a small current density with a large statistical error.

As in the case of EMD diffusivity, the decrease of conductivity in small pores is expectedly caused by inhomogeneity in the pore. To investigate whether there is any changes in the nonequilibrium radial distribution of ions under the electric field, the steady-state radial density profiles in the NEMD are

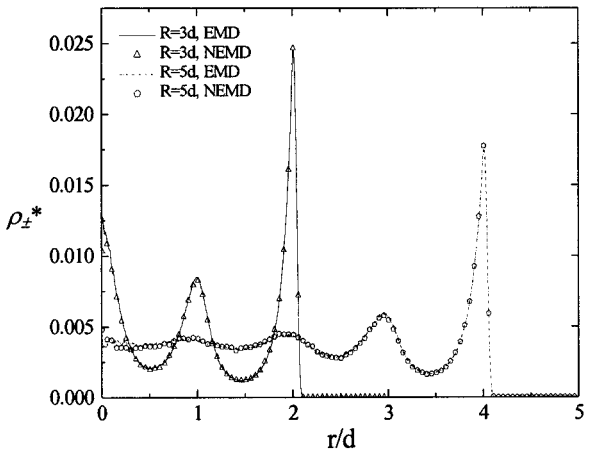

Figure 4. Comparison of radial distributions of ions in NEMD and EMD simulations at $\eta_s = 0.3$ solvent packing fraction.

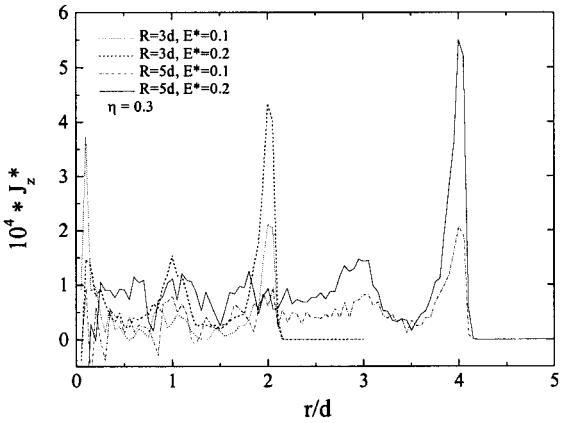

Figure 5. Current density distributions inside cylindrical pores for SPM at $\eta_s = 0.3$ solvent packing fraction and different pore sizes and field strengths obtained by NEMD simulations.

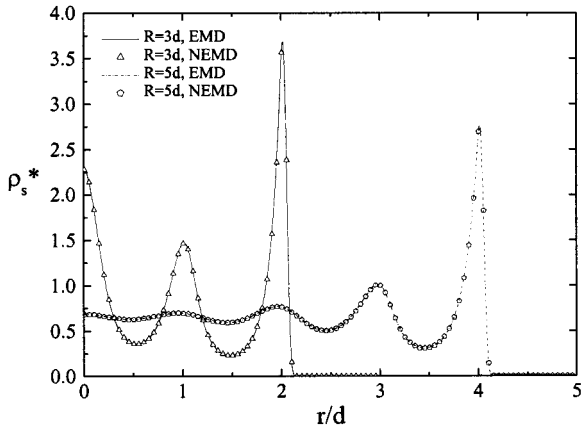

Figure 6. Comparison of distributions of solvent molecules inside cylindrical pores In NEMD and EMD simulations at $\eta_s = 0.3$ solvent packing fraction.

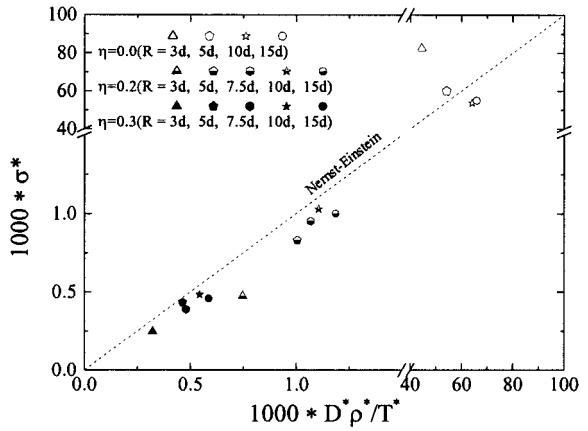

Figure 7. Nernst−Einstein plot of electric conductivity vs diffusion coefficient of ions. The electric conductivity is obtained from NEMD simulations, while the diffusion coefficient is obtained from EMD simulations.

calculated. Figure 4 shows the density profiles in two small pores, and the results are compared with the EMD density profiles. It is unambiguous that the concentration distributions are the same. The radial distribution of current density is also calculated for each pore size. The results for two small pore sizes are shown in Figure 5. For clarity, only data at two reduced field strengths $E_z^* = 0.1$ and 0.2 are shown. High current peaks can be found at the location of the physical radius and roughly correlate to the density profiles in Figure 4. While fluctuations in the current profiles exist, particularly near the center of the pore, the heights of peaks are in general proportional to the amplitude of the applied field strength. The correlation of higher local current density to local density of ions can be understood since the higher local concentration of ions give a higher ion flux, with everything being equal. However, the density peaks of ions and solvents shown in Figure 6 are at the same location. The higher local solvent density will not contribute to current but will increase the frictional resistance significantly for the local ion flux. In a comparison of the profiles in Figures 4, the density peak at the pore wall is higher for $R = 3$ than $R = 5$, due to increased confinement. The corresponding current density peak for $R = 3$ in Figure 5, however, is lower than that for $R = 5$. It can be explained that, in the high-density layers, the ions collide many more times with solvent molecules than in the low-density layers and therefore the current density does not increase in proportional to the density of the layer.

Since the early publications of Nernst and Einstein, it is well-known that the electric conductivity of ions in a solvent is not independent of their diffusion coefficients. Apart from the case of RPM with $\eta_s = 0$, the curves in Figures 2 and 3 show the same trend and correlate to each other. A closer examination of the validity of the Nernst−Einstein relation is made by calculating the reduced electric conductivity of ions from their diffusion coefficients obtained by EMD simulations using eq 13. These calculated electric conductivities are tabulated in Table 3 and compared with those obtained from NEMD in the last column of Table 3. This comparison can be illustrated graphically in Figure 7 with the validity of the Nernst−Einstein relation confirmed by data points falling on the 45° line. Except for the few cases of smallest pores in the RPM model, the data points in Figure 7 fall below the 45° line. This indicates that confine effect may be more significant on the migration in NEMD simulations than on the diffusion in EMD simulations. In a comparson of the results of the SPM model at two densities, larger deviations from the Nernst−Einstein relation are observed for $\eta_s = 0.2$. This is due to the larger importance of particle−wall interaction versus particle−particle interaction in the case of a lower packing fraction. For the case of $\eta_s = 0.3$, the data points fall close to the 45° line except for the smallest pore size. The largest deviation is found for $R = 3d$ in both packing fractions, indicating the confinement effect on the validity of the Nernst−Einstein relation. For an electrolyte with a realistic packing fraction, the Nernst−Einstein relation may be acceptable for pores larger than $R = 5d$, but the prediction by the EMD overestimates the conductivity in a nanopore smaller than $R =$

5d. The exceptional case is the RPM where the EMD approach underestimates the conductivity for several cases of small pore sizes. As explained earlier, this is due to the change of Columbic interaction which plays a larger role in the absence of solvent friction. As far as the proximity of the SPM model being a more realistic representative of the electrolyte, we can expect that failure of the Nernst−Einstein relation in small nanopores due to confinement effects. This will cast some doubts to the general approach of extrapolating EMD diffusion coefficients for nonequilibrium current situations.

The effect of concentration on the validity of the Nernst−Einstein relation is well understood in the literature. We have chosen only one concentration of 0.1 M in the simplest molecular solvent model to explore the confinement effect on the Nernst−Einstein relation. More refined investigations should be made in the future, e.g. for the confinement effects at other concentrations. We have also made the artificial assumption of a constant 0.1 M equilibrium concentration in the pores of various sizes. In reality, a more concentrated external solution is needed to be in equilibrium with a 0.1 M solution inside the pore. For a 1:1 SPM model external solution at 0.1 M and $\eta_s = 0.3$, the equilibrium concentration inside an $R = 5.0d$ uncharged pore is 0.0745 M, as determined by a grand canonical Monte Carlo (GCMC) simulation.[40] In this study, the internal concentration is fixed for convenience. It will be more logical to use the external solution concentration as a reference, for example at 0.1 M, by fixing the chemical potential and performed a GCMC simulation for each pore size to determine the corresponding internal concentration. It is expected that the internal concentration will be lower in smaller pores and there will be a further decrease in current due to fewer charge carriers. The confinement effects on conductivity and deviations from Nernst−Einstein relation will be larger than what are observed here with a constant internal concentration. NEMD simulations with the true concentration of electrolyte in equilibrium to a bulk liquid of 0.1 M concentration is warranted, and grand canonical Monte Carlo simulations results such as those reported earlier will be useful.[5,8−12,14]

The desire for a more realistic model of water is obvious. The SPM model improves over the RPM model with a realistic packing. The effect of confinement on solvation of ions and orientation of solvent molecules cannot be explored in details with the present SPM model. Lynden-Bell and Rasaiah[20] found that small ions tended to lie away from the pore walls because the lower energy in a solvated structure. The present results of SPM, however, see ions and currents near the walls. In addition, the assumption of a uniform dielectric constant is also problematic at the wall and electrostatics have to be worked out to arrive at the correct boundary conditions. Using a multipolar water model can alleviate this problem of boundary conditions. We have not studied the SPM model electrolyte in pores smaller than $R = 3d$. The need of a better model of solvent is more apparent in the extremely narrow pores.

The present study focuses on NEMD simulations with a steady-state direct current. Relaxation phenomenon and frequency-dependent conductivity in a nanopore are of interest in many applications. NEMD simulations of ionic migration under an alternating electric field have been started with the RPM model,[41] and extensions to more realistic solvent models will be of interest.

Summary

We have reported equilibrium and nonequilibrium molecular dynamics simulation study of a solvent primitive model electrolyte confined in nanopores. The diffusivity and conductivity of a 0.1 M 1:1 electrolyte are calculated for pores ranging from 3 to 15 times the diameter of the ion. Similar values of diffusivity and conductivity are found in large pores were close to bulk electrolyte behavior as expected. For pores smaller than 5 times the diameter of the ion, the diffusion coefficient and conductivity decreases with decreasing pore radius, due to increasing inhomogeneity. These confinement effects correlate with the density profiles and radial distribution of current density. For the restricted primitive model electrolyte where packing of solvent is absent, an increase in conductivity was observed due to weakening of average Columbic interaction in a linear geometry. The validity of the Nernst−Einstein relation is explored in the nanopores by comparing the conductivities obtained by nonequilibrium simulations and those calculated from equilibrium diffusion coefficients. While the failure of the Nernst−Einstein relation due to ion−ion interactions at high concentration is often addressed, the failure due to confinement effects is discussed here for the first time. From the results of the present study, the conductivities calculated from equilibrium molecular dynamics simulations are lower than the results of NEMD simulations. The general approach of extrapolating the EMD results to nonequilibrium simulation may have some limitations for very small pores.

Acknowledgment. Financial support from the Research Grants Council of Hong Kong (HKU 7213/99P) and the Hungarian National Research Fund (OTKA-T025884) is acknowledged.

References and Notes

(1) Thommes, M.; Kohn, R.; Froba, M. *J. Phys. Chem.* **2000**, *104*, 7932.
(2) Nicholson, D.; Parsonage, N. G. *Computer Simulation and the Statistical Mechanics of Adsorption*; Academic Press: San Diego, CA, 1982. Gelb, L. D.; Gubbins, K. E. *Langmuir* **1998**, *14*, 2097.
(3) Heffelfinger, G. S.; van Swol, F.; Gubbins, K. E. *Mol. Phys.* **1987**, *61*, 1381.
(4) Davis, H. T. *J. Chem. Phys.* **1987**, *86*, 1474.
(5) Vlachy, V.; Haymet, A. D. J. *J. Am. Chem. Soc.* **1989**, *111*, 477; *J. Electroanal. Chem.* **1990**, *283*, 77.
(6) Jamnik, B.; Vlachy, V. *J. Am. Chem. Soc.* **1993**, *115*, 660.
(7) Hribar, B.; Vlachy V.; Bhuiyan, L. B.; Outhwaite C. W. *J. Phys. Chem. B* **2000**, *104*, 11522.
(8) Lo, W. Y.; Chan, K. Y. *Mol. Phys.* **1995**, *86*, 745.
(9) Lee, M.; Chan, K. Y. *Chem. Phys. Lett.* **1997**, *275*, 56.
(10) Rivera, S.; Sorenson, T. S. *Mol. Simul.* **1994**, *13*, 115.
(11) Sorensen, T. S.; Sloth, P. *J. Chem. Soc., Faraday Trans.* **1992**, *88*, 571.
(12) Lo, W. Y.; Chan, K. Y.; Lee, M.; Mok, K. L. *J. Electroanal. Chem.* **1998**, *450*, 265.
(13) Boda, D.; Busath, D. D.; Henderson, D.; Sokolowski, S. *J. Phys. Chem. B* **2000**, *104*, 8903.
(14) Lee, M.; Chan, K. Y.; Nicholson, D.; Zara, S. *Chem. Phys. Lett.* **1999**, *307*, 89.
(15) Steck, A.; Yeager, H. L. J. *Electrochem. Soc.* **1983**, *130*, 1297.
(16) Gavach, C.; Pamboutzoglou, G.; Nedyalkov, M.; Poucelly, G. *J. Membr. Sci.* **1989**, *45*, 37.
(17) Westermann-Clark, G. B.; Anderson, J. L. *J. Electrochem. Soc.* **1983**, *130*, 839.
(18) Hansma, P. K.; Drake, B.; Marti, O.; Gould, S. A. C.; Prater, C. B. *Science* **1989**, *243*, 641.
(19) Sackmann, B.; Neher, E. *Single Channel Recording*; Plenum: New York, 1995.
(20) Lynden-Bell, R. M.; Rasaiah, J. C. *J. Chem. Phys.* **1996**, *105*, 9266.
(21) Smith, G. R.; Sansom, M. S. P. *Biophys. J.* **1997**, *73*, 1364.
(22) Eisenberg, R. S. *Acc. Chem. Res.* **1998**, *31*, 117.
(23) Svishchev, I. M.; Kusalik, P. G. *Physica A* **1993**, *192*, 628.
(24) Svishchev, I. M.; Kusalik, P. G. *Phys. Chem. Liq.* **1994**, *26*, 237.
(25) Tang, Y. W.; Szalai, I.; Chan, K. Y. *Mol. Phys.* **2001**, *99*, 309.
(26) Tjatjopoulos, G. J.; Feke, D. L.; Mann, J. A. *J. Chem. Phys.* **1988**, *92*, 4006.

(27) Wang, Z. X.; Guo, D. R. *Special Functions*; World Scientific: Singapore, 1989.
(28) Rapaport, D. C. *The Art of Molecular Dynamics Simulation*; Cambridge University Press: New York, 1995.
(29) MacElroy, J. M. D.; Suh, S.-H. *Mol. Phys.* **1987**, *60*, 475.
(30) Heffelfinger, G. S.; van Swol, F. *J. Chem. Phys.* **1994**, *100*, 7548.
(31) Evans, D. J.; Morriss, G. P. *Statistical Mechanics of Nonequilibrium Liquids*; Academic Press: London, 1990.
(32) Evans, D. J.; Morriss, G. P. *Comput. Phys. Rep*. **1984**, *1*, 297.
(33) Crozier, P. S.; Rowley, R. L.; Holladay, N. B.; Henderson, D.; Busath, D. D. *Phys. Rev. Lett.* **2001**, *86*, 2467.
(34) Heyes, D. M. *The Liquid State (Application of Molecular Simulations)*; John Wiley & Sons: Chichester, U.K., 1997.
(35) Heyes, D. M. *Phys. Rev. B* **1988**, *37*, 5677.
(36) Nernst, W. *Z. Phys. Chem.* **1888**, *2*, 613; **1889**, *4*, 129.
(37) Planck, M. *Ann. Phys. Chem.* **1890**, *39*, 161.
(38) Vanderlick, T. K.; Davis, H. T. *J. Chem. Phys*. **1987**, *87*, 1791.
(39) Henderson, D. *Fundamentals of Inhomogeneous Fluids*; Marcel Dekker: New York, 1992.
(40) Lee, M. Ph.D. Thesis, The University of Hong Kong, 2000.
(41) Tang, Y. W.; Szalai, I.; Chan, K. Y. Submitted for publication in *Mol. Phys.*